rev2025 Resource Efficient Vehicles Conference 23 – 25 September 2025

Optimizing energy consumption of regional trains through speed adjustment: a seasonal and regional perspective

Amir Torkiharchegani[1,*], Marcel Scharmach[2], Mats Alaküla[1], Rickard Persson[3], Libor Lochman[4], Christoffer Ahrling[5], Martin Tunér[5]

[1] *Division of Industrial Electrical Engineering and Automation, LTH, Faculty of Engineering, Lund University, Lund, Sweden.*
[2] *Institute of Vehicle Concepts, German Aerospace Center, Stuttgart, Germany.*
[3] *Department of mechanical engineering, KTH Royal Institute of Technology, Stockholm, Sweden.*
[4] *Wabtec Corporation, Rome, Italy.*
[5] *Department of Energy Sciences, Lund University, Lund, Sweden*
[*] *Corresponding author. amir.torkiharchegani@iea.lth.se*

ABSTRACT

Efficient energy management is a key challenge for regional train services, especially when considering the seasonal variation in auxiliary energy demands such as heating, ventilation, and air conditioning (HVAC). This study explores how adjusting the maximum operational speed of regional trains can optimize energy consumption without exceeding design limits or necessitating larger battery sizes. By achieving a balance between train speed, available travel time, and seasonal auxiliary energy needs, the study proposes an approach to enhance sustainability and reduce operational costs. The research begins by modelling HVAC energy demands under different climatic conditions and train capacities. Using this model, energy consumption for a battery-powered regional train is simulated on two distinct routes: each with unique drive profile and timetables. The simulations are conducted using MATLAB, considering the impact of speed adjustments on both traction energy and auxiliary energy requirements. Results demonstrate the significant potential of speed adjustments to reduce total energy consumption. This approach ensures that battery sizes remain manageable while maintaining performance

https://doi.org/10.25364/978-3-903374-48-5_22

standards across different routes and timetables. Furthermore, the findings highlight the broader implications of speed adjustment on battery lifecycle, and CO_2 emissions. This research underscores the importance of precise speed adjustments in achieving optimal performance, cost-effectiveness, and sustainability in regional rail services.

1. INTRODUCTION

The transportation sector remains one of the most significant contributors to global greenhouse gas (GHG) emissions, and although rail transport is among the most efficient modes in terms of energy use per passenger-kilometre, many regional networks still rely on diesel multiple units (DMUs). In light of the European Union's climate goals, such as the European Green Deal target to reduce transport emissions by 90% by 2050, transitioning to cleaner technologies is essential [1].

Battery Electric Multiple Units (BEMUs) are gaining momentum as a sustainable alternative to DMUs on non-electrified or partially electrified rail lines. These trains offer several environmental and operational benefits: zero local emissions, lower noise levels, and compatibility with renewable electricity sources. Notable examples include the Stadler FLIRT Akku, and the Siemens Mireo Plus B, which are optimized for regional and commuter applications [2], [3]. Nevertheless, the widespread adoption of BEMUs is not without challenges. Key concerns include the limited energy capacity of onboard batteries, long recharging times, and high energy demand from auxiliary systems, especially under extreme seasonal conditions.

One of the primary auxiliary energy consumers is the heating, ventilation, and air conditioning (HVAC) system. Depending on climate and passenger occupancy, HVAC loads can represent a substantial portion of total energy consumption. In winter, heating demands spike; in summer, cooling must compensate for solar heat gain and high occupancy levels. Efficient control of HVAC loads is therefore crucial to ensuring energy availability for traction, extending battery life, and maintaining operational reliability. A viable strategy to address these challenges lies in speed optimization.

This study proposes a practical and scalable solution: regulating the train's maximum operational speed in accordance with seasonal HVAC demands and route characteristics. Rather than increasing battery capacity, which adds mass, cost, and environmental burden, adjusting speed can reduce traction energy consumption during periods of high auxiliary load, thus balancing the total energy budget. This strategy is particularly effective when coordinated with flexible timetables, and it avoids the need for route-specific train designs.

The analysis presented in this paper uses MATLAB-based simulations to investigate two regional train routes with varying drive profiles, stop frequencies, and terrain conditions. The study models HVAC energy demand using standardised operating points, applies a thermal load profile, and battery degradation modelling via Rainflow analysis. The resulting insights include the impact of speed adjustment on total energy consumption, battery cycle life, operational costs, and CO_2 emissions.

The remainder of this paper is structured as follows: Section 2 presents the simulation methodology, including vehicle specifications, route profiles, and modelling assumptions. Section 3 provides the results of the simulations and discusses their implications. Section 4 concludes the paper and offers recommendations. The final sections include acknowledgements and references.

2. METHODOLOGY

This section outlines the simulation methodology used to assess the impact of seasonal speed adjustment on the energy performance of battery-electric regional trains. It includes route selection, train configuration, modelling of traction and auxiliary energy demand, and battery life estimation under dynamic operating conditions.

Two regional routes with contrasting characteristics are selected as case studies. The first route A, between Delmenhorst and Harpstedt in Germany, is 42 km long and includes 8 stops. The second route B connects Borlänge to Malung in Sweden, spanning 129 km with 12 intermediate stops. Both routes are simulated as round trips, with elevation, velocity, and timing profiles derived from geographic and timetable data. These profiles are illustrated in Figure 1.

The train is powered by a 390 kW electric traction machine, has a gross vehicle mass of 30 tons, 15 meters length, and 10 square meters front area. For energy storage, two battery configurations are considered: a 550 kWh system for the longer Swedish route and a 175 kWh system for the shorter German route. Both configurations are sized to accommodate full daily service without exceeding a critical depth of discharge threshold.

Traction energy demand is calculated using the Davis equation ($R_{Rolling} = 400+2v+0.2v\text{^}2$; v is velocity in km/h), which includes rolling, aerodynamic, and acceleration resistances. The effect of terrain is incorporated through a

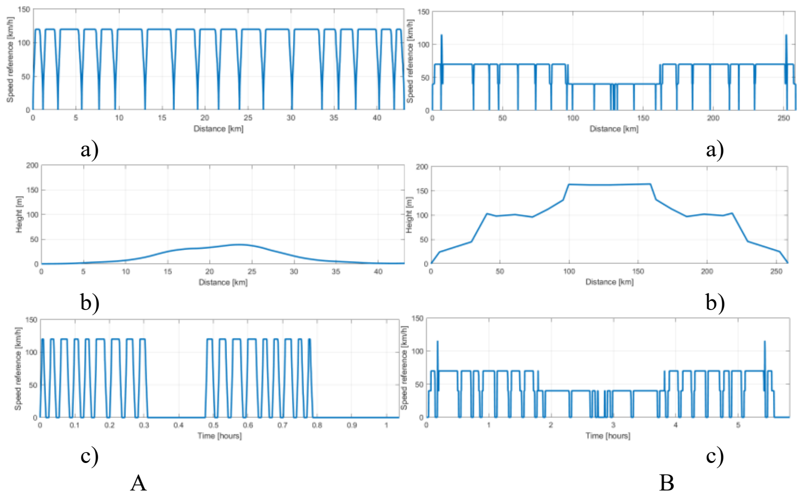

Figure 1: a) Distance-speed, b) distance-elevation, and c) velocity-time profiles for round-trip Route A and Route B.

gradient resistance term $R_{gradient}=M\cdot g\cdot \sin(\theta)$ (M is the train mass, g gravitational acceleration, and θ is the road gradient derived from the elevation profile.), dynamically computed from the elevation profile for each simulation time step. The total resistance R_{total} is then converted into traction force, and multiplied by velocity (converted to m/s) to compute instantaneous traction power ($P=R_{total}\cdot v$). This power value is used to determine the required motor torque based on drive train speed and efficiency. The traction system includes a 390 kW permanent magnet synchronous motor (PMSM), with performance evaluated using its torque-speed efficiency map.

To evaluate the potential of speed-based optimization, each route is simulated with varying speed scaling factors. For Route A, the scaling range is 0.6 to 1.0. Dwell time at stations remains constant, and changes in speed affect only cruise segments. This approach enables investigation into the trade-offs between traction energy, auxiliary loads, and journey time. For Route B, maximum speed is scaled between 0.8 and 1.2 (relative to a baseline of maximum speed at each moment).

Auxiliary energy demand, particularly for HVAC systems, is modelled based on a 1D thermal simulation developed within the Flagship Project 6: FutuRe project [4]. This model incorporates temperature and humidity control, solar radiation, and passenger-generated heat and humidity. Simulations are performed under both static ($v = 0$) and dynamic ($v > 0$) conditions. No energy

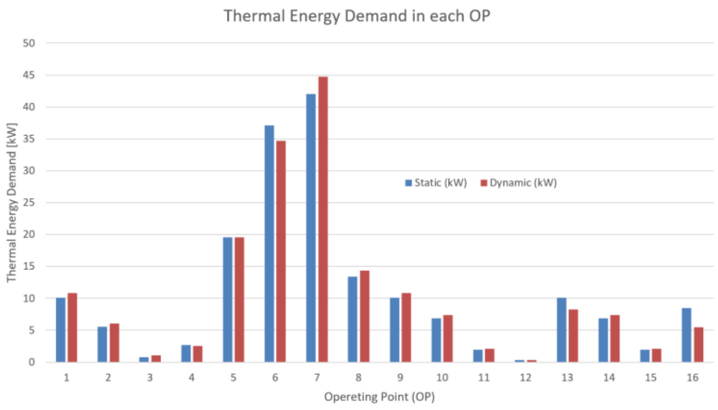

Figure 2: Thermal energy demand in static vs. dynamic conditions across 16 operating points.

contribution from fans or compressors is considered, and the coefficient of performance (COP), defined as the ratio of useful heating or cooling output to the electrical energy input, is fixed at 1 to represent a worst-case scenario with no efficiency gain from HVAC systems.

Sixteen standardized operating points (OPs), developed in alignment with DIN EN 50591 and DIN EN 14750-1 Class A, are used to parameterize external conditions such as ambient temperature, relative humidity, and passenger occupancy (ranging from 0 to 120 passengers), which also affects traction energy demand. These OPs reflect realistic seasonal and occupancy variations. Table 1 summarises the environmental parameters for each OP.

Thermal energy demand for each OP is simulated for both static and dynamic modes. Results indicate that peak demands (up to ~45 kW) occur during summer scenarios with full occupancy (e.g., OP6 and OP7), while winter scenarios with no passengers present minimal HVAC loads. These findings are illustrated in Figure 2.

Thermal energy demand for each OP is simulated under both static and dynamic conditions. For simplification, a fixed coefficient of performance (COP) of 1 is applied for both heating and cooling to represent worst-case scenarios. In practice, cooling systems typically operate with a COP of around 2, while heating remains closer to 1. Based on this, worst-case HVAC demands are assumed for summer cooling with full occupancy, and winter heating. These results are illustrated in Figure 2.

To evaluate battery aging, a Rainflow counting algorithm is applied to the time-series state-of-charge (SOC) profile of the battery under each speed scenario. A cycle-life curve is used to estimate the service life as a function of the depth of discharge [5], [6]. The assumption is based on continuous daily operation (24/7).

Together, this simulation framework provides a comprehensive basis for assessing the trade-offs between maximum speed, total energy consumption, battery degradation, and HVAC performance under seasonally varying conditions.

3. RESULTS

This section presents and analyses the simulation results based on adjusted drive profiles, energy consumption, auxiliary load effects, battery degradation, and the associated economic

and environmental impacts. All results are derived from MATLAB-based simulations that implement drive cycles, elevation data, and HVAC operating points, as described in Section 2.

Speed adjustments were implemented via a scaling factor applied to the original velocity profile. These factors range from 0.6 to 1.0 for Route A and 0.8 to 1.2 for the route B. The simulations confirm that all scaled profiles respect constraints: dwell times at stations remain unchanged, and speed never exceeds the design limit of 120 km/h. The adjusted profiles allow full route completion.

Table 1: Operating points including temperature, humidity, and passenger load conditions.

Operating Point	Temperature (°C)	Humidity (%)	Passengers (%)
OP1	-10	90	0
OP2	0	90	100
OP3	10	90	50
OP4	15	90	50
OP5	22	80	100
OP6	28	70 (I), 70 (II),45 (III)	100
OP7	40 (I), 35 (III), NA (III)	40 (I), 50 (II), NA (III)	100
OP8	NA (I), -20 (II), -40 (III)	90	0
OP9	-10	90	0
OP10	0	90	0
OP11	15	80	0
OP12	22	80	0
OP13	40 (I), 35 (II), 28 (III)	40 (I), 40 (II), 70 (III)	0
OP14	0	90	0
OP15	15	80	0
OP16	28	50	0

3.1 ENERGY DEMAND AND SPEED ADJUSTMENT UNDER AUXILIARY LOAD SCENARIOS

Figures 3 and 4 illustrate how changes in maximum train speed affect three key variables for each route: total energy consumption, auxiliary energy consumption, and total travel time, under a range of assumed HVAC loads (0 to 45 kW). In this study, HVAC demand is used as a proxy for overall auxiliary consumption, with the understanding that other consumers such

as lighting, door mechanisms, and control systems are present but assumed constant throughout all scenarios. Figure 2 provides the basis for HVAC load variation across operating points.

Figure 3 illustrates the variation in total energy consumption, auxiliary (HVAC) energy use, and travel time under different speed scaling factors for route A. When the maximum speed is reduced by up to 40%, the total travel time increases by approximately 30% (Figure 3c). Despite this time extension, substantial energy savings are observed, especially in high auxiliary power conditions. As shown in Figure 3a, the total energy demand drops by 30 to 50 kWh, depending on the HVAC power level.

The magnitude of energy savings is strongly influenced by the auxiliary load. Figure 3b shows that at higher HVAC levels, such as 45 kW, the auxiliary energy demand remains high, while the impact of speed change on traction energy becomes more noticeable. This is why the benefit of speed reduction is more significant at higher HVAC loads. Nevertheless, HVAC is not the only influencing factor: when total energy demand is lower, battery charging and discharging losses are also reduced, leading to additional efficiency gains. This effect is embedded in the simulation model through internal power electronics loss modeling.

Assuming an average total energy demand of 100 kWh per round trip, the data show that under this level, all auxiliary power levels from 0 to 45 kW can be accommodated within the same battery capacity. This suggests the following strategy:

- With low HVAC demand, trains can follow original speed profiles within energy limits.
- With high HVAC demand, reduction of the maximum speed helps balance auxiliary energy use.

It should be noted that these results are specific to the train configuration defined in Section 2, including a 390 kW permanent magnet synchronous motor (PMSM). The motor's energy consumption is computed based on an efficiency map depending on operating torque and speed, although the efficiency diagram is not included in this paper. The power electronic motor drive and the mechanical transmission are both modelled with constant efficiencies.

A similar analysis for the longer route B is shown in Figure 4. Although speed changes are more limited in this case (±20%), the trends are consistent. Due to the longer distance, different number of stops per unit, and distinct drive profile and topography, the effect of the maximum speed changes is less pronounced. As shown in Figure 4a, the difference in total energy consumption across the maximum speed range is smaller, yet still present. This is because the longer travel duration amplifies the influence of HVAC runtime on total consumption. In high-load scenarios (e.g., 45 kW), HVAC power can represent more than 50 % of the total energy use.

While energy savings are relatively smaller on this route, the results still support using speed adjustment as a lever for matching HVAC load to battery capacity. For example:

- At low HVAC loads, reducing speed improves energy efficiency by lowering traction demand.
- At high HVAC loads, prolonged HVAC operation may outweigh traction savings, making higher speeds preferable when minimizing travel time is important.

Overall, for this track, the original drive profile appears suitable for average seasonal conditions, but adaptive speed control is recommended under more demanding HVAC scenarios.

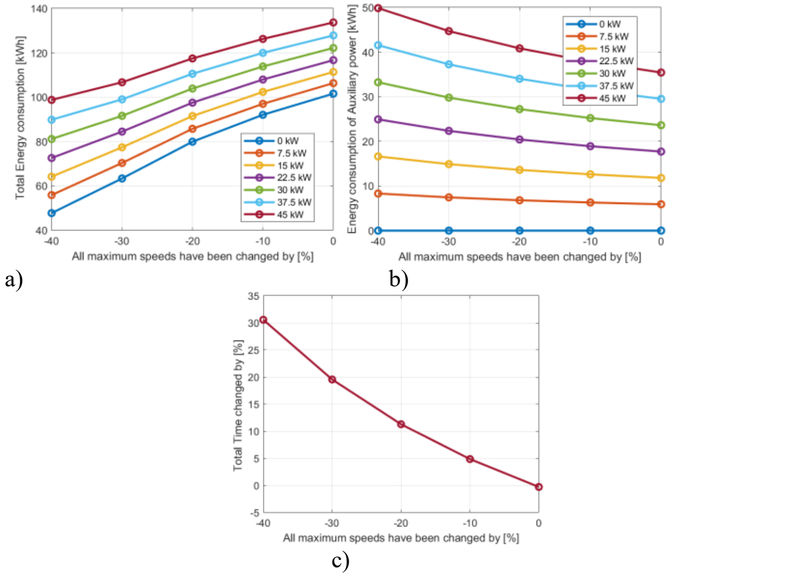

Figure 3. Total energy consumption (a), auxiliary energy consumption (b), and travel time variation (c) for route A under various speed scaling factors and HVAC power levels.

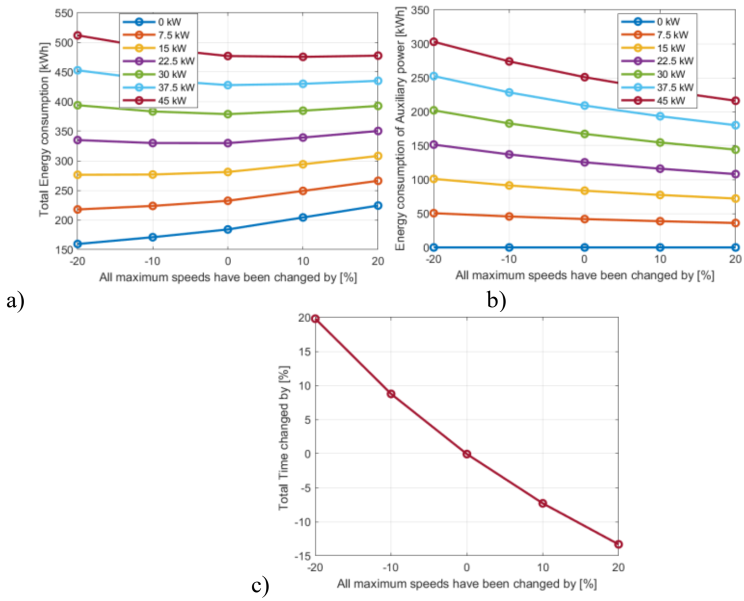

Figure 4. Total energy consumption (a), auxiliary energy consumption (b), and travel time variation (c) for route B under various speed scaling factors and HVAC power levels.

3.2 BATTERY DEPTH OF DISCHARGE AND SERVICE LIFE

Figure 5 illustrates the relationship between speed adjustment, depth of discharge (DoD), and battery lifetime for route A. As shown in Figure 5a, it is observed that reducing the maximum speed by up to 40 % results in a significant decrease in DoD, ranging from 20 % to 30 % across different levels of auxiliary power. The depth of discharge increases consistently with higher auxiliary loads and higher speeds.

The impact of this variation on battery lifetime is shown in Figure 5b. A degradation model based on Rainflow counting and DoD-dependent cycle life is applied, assuming continuous operation (24 hours a day, 365 days a year). Although real-world trains often experience fewer daily cycles and longer calendar life, a conservative maximum battery service life of 20 years is considered here [7].

Under scenarios with the lowest auxiliary power, adjusting the maximum speed can increase the battery life from approximately 3 years to over 14 years. Even at 45 kW auxiliary load, which represents a worst-case HVAC scenario, lifetime still improves from about 2 to 5 years by applying speed reduction. These results indicate that maximum speed adjustment can significantly extend the time before battery replacement is needed, even under demanding conditions. Based on an average battery cost of €100 per kWh [8], increasing battery longevity directly reduces replacement costs and lowers the total cost of ownership. Moreover, longer lifetime reduces the frequency of battery production and disposal, contributing to sustainability goals. These results support the integration of speed planning not only for energy management but also as a strategy for battery aging mitigation and cost control.

For the longer route B, similar analyses are presented in Figure 6. Figure 6a shows that changes in DoD are generally smaller across the speed range (–20 % to +20 %), due to the higher initial energy demand and larger installed battery capacity. Nevertheless, a noticeable trend remains. The corresponding impact on lifetime is shown in Figure 6b. For example, at 25 kW auxiliary power, battery service life ranges from approximately 15 to 20 years, depending on the maximum speed. However, at low auxiliary loads, the battery already reaches its calendar life limit of 20 years, and further reductions in speed no longer yield lifetime benefits. At very high auxiliary loads (e.g., 45 kW), the influence of speed becomes marginal due to the dominant effect of HVAC energy demand.

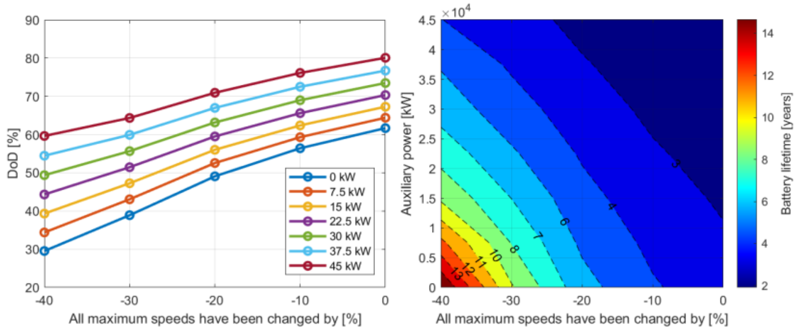

a) b)

Figure 5. (a) DoD for the route A under different maximum speed levels and auxiliary power conditions (0 to 45 kW). (b) Estimated battery lifetime under the same conditions.

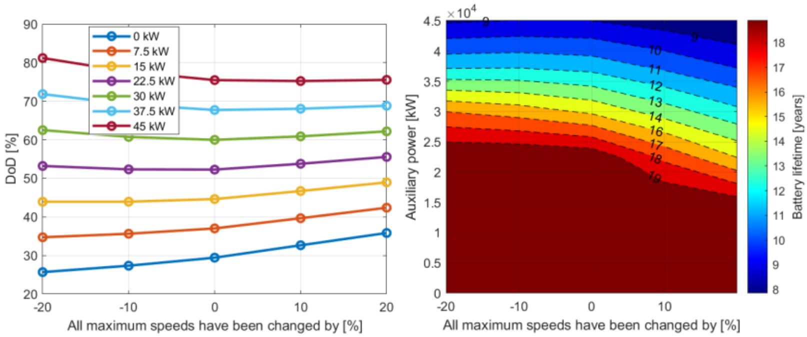

a) b)

Figure 6. (a) DoD for the route B across varying auxiliary power levels and speed scaling (–20 % to +20 %). (b) Estimated battery lifetime under the same conditions.

3.3 ECONOMIC AND ENVIRONMENTAL IMPACT

The economic and environmental implications of speed adjustment strategies are evaluated in Figures 7 and 8, based on variations in auxiliary power levels and grid emissions. Using an average electricity price of €0.28 per kilowatt-hour for Sweden and Europe in 2023[9], [10], the electricity cost per kilometre was calculated for both simulated routes. For route A, Figure 7a shows that this cost varies significantly depending on speed and auxiliary demand. Similarly, for the route B, Figure 8a demonstrates that costs range.

The associated environmental impacts are presented in terms of CO_2 emissions per kilometre, calculated for two grid contexts. For Sweden, one of Europe's cleanest electricity producers, the emission intensity is 26.5 gCO_2eq/kWh on average (2019–2023)[11]. In contrast, the European grid average is significantly higher, at 244 gCO_2eq/kWh (2019–2022)[12]. In Figure 7b, emissions for the shorter route A range under the European average. Similarly, Figure 8b indicate emissions for Sweden along the route B.

These results emphasize that energy-efficient operation, achieved through the maximum speed adjustment, has not only a measurable impact on electricity cost but also a considerable influence on transport-related carbon emissions, particularly in regions with fossil-heavy electricity production. Furthermore, these benefits extend beyond operation. As discussed in Section 3.3, reducing energy consumption and extending battery life decreases the need for frequent battery replacement, which also reduces upstream CO_2 emissions from battery manufacturing. Given that the carbon footprint of lithium iron phosphate (LFP) battery production is approximately 55 kg CO_2eq per kilowatt-hour[13], any operational strategy that reduces battery usage or size contributes to lifecycle sustainability.

In summary, seasonal speed adjustment strategies offer a promising approach for reducing both operational costs and environmental impact in battery-electric train services. While the effectiveness of this method is particularly pronounced under high auxiliary loads, elevated electricity prices, or carbon-intensive energy grids, the authors acknowledge that any real-world implementation must be accompanied by comprehensive safety assessments, revised operational protocols, and route-specific feasibility analyses. These considerations do not diminish the value of the findings; rather, they emphasize the importance of further research and coordination with regulatory frameworks to ensure that the substantial potential benefits identified in this study can be safely and practically realized.

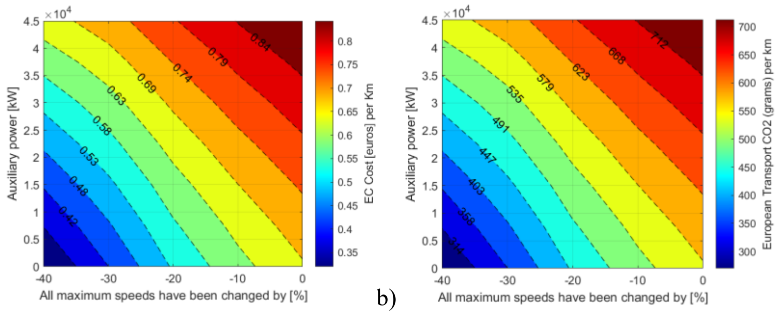

a) b)

Figure 7. (a) Electricity cost per kilometre for route A across speed and auxiliary power levels. (b) CO_2 emissions per km assuming the European grid average

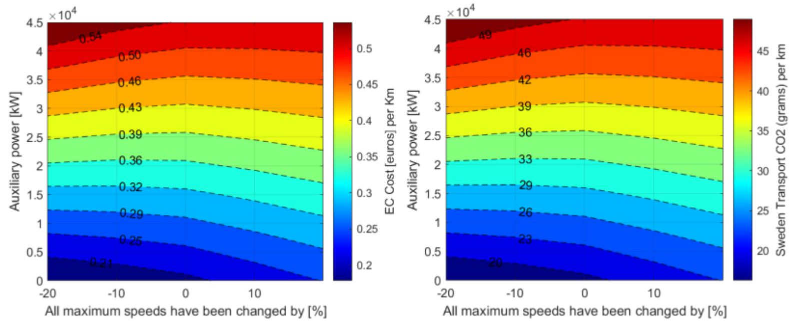

a) b)

Figure 8. (a) Electricity cost per kilometre for route B across speed and auxiliary power levels. (b) Transport-related CO_2 emissions for Sweden

4. CONCLUSION

This study demonstrates that seasonal adjustment of the maximum speed provides a practical and efficient approach to improve the energy performance, battery lifetime, and environmental footprint of battery-electric regional trains. By aligning operational speed with auxiliary energy demands, minimize battery degradation, and lower CO_2 emissions without altering hardware or battery capacity.

Importantly, the results showed that the effectiveness of seasonal adjustment of maximum speed varies between cases, depending on route characteristics, train specifications, and auxiliary load profiles. Therefore, any implementation must be evaluated case-by-case, considering local topology, service frequency, and vehicle configuration. Although practical deployment requires alignment with safety protocols, timetable constraints, and regulatory frameworks, the demonstrated benefits justify further investigation and application.

ACKNOWLEDGEMENTS

This project received funding from the European Union's Horizon Europe, Europe's Rail JU under grant agreement No. 101101962 (FP6 FutuRe). The views expressed are those of the authors and do not necessarily reflect those of the European Union or Europe's Rail.

REFERENCES

[1] E. COMMISSION. "Sustainable and Smart Mobility Strategy – putting European transport on track for the future." https://eur-lex.europa.eu/legal-content/EN/TXT/?uri=CELEX:52020DC0789.

[2] STADLER. "Lightweight and flexible: FLIRT." https://www.stadlerrail.com/en/solutions/rolling-stock/mainline-flirt.

[3] SIEMENS. "Mireo Plus B – A pioneering step into the future." https://www.mobility.siemens.com/global/en/portfolio/rolling-stock/commuter-and-regional-trains/mireo/mireo-plus-b.html.

[4] FP6_FutuRe. "Flagship Project 6: FUTURE - Delivering innovative rail services to revitalise capillary lines and regional rail services." Europe's Rail. https://projects.rail-research.europa.eu/eurail-fp6/.

[5] p. tumblr. "lithium & solar power LiFePO4." https://gwl-power.tumblr.com/post/130701906811/faq-lifepo4-cycle-life-based-on-dod-the-graph.

[6] Y.-S. Cheng, Y.-H. Liu, H. C. Hesse, M. Naumann, C. N. Truong, and A. Jossen, "A pso-optimized fuzzy logic control-based charging method for individual household battery storage systems within a community," *Energies,* vol. 11, no. 2, p. 469, 2018.

[7] ANL. "EV BATTERIES AND RECYCLING." Argonne National Laboratory. https://www.anl.gov/esia/reference/ev-batteries-and-recycling.

[8] BloombergNEF. "Lithium-Ion Battery Pack Prices Hit Record Low of $139/kWh." https://about.bnef.com/blog/lithium-ion-battery-pack-prices-hit-record-low-of-139-kwh/.

[9] eurostat. "Electricity and gas prices stabilise in 2023." https://ec.europa.eu/eurostat/web/products-eurostat-news/w/ddn-20231026-1.
[10] eurostat. "Electricity price statistics." https://ec.europa.eu/eurostat/statistics-explained/index.php?title=Electricity_price_statistics#:~:text=The%20EU%20average%20price%20in,was%20%E2%82%AC0.2847%20per%20KWh.
[11] Nowtricity. "CURRENT EMISSIONS IN SWEDEN." https://www.nowtricity.com/country/sweden/.
[12] EEA. "Greenhouse gas emission intensity of electricity generation." European Environment Agency. https://www.eea.europa.eu/data-and-maps/daviz/co2-emission-intensity-15#tab-chart_7.
[13] J. A. Llamas-Orozco *et al.*, "Estimating the environmental impacts of global lithium-ion battery supply chain: A temporal, geographical, and technological perspective," *PNAS nexus,* vol. 2, no. 11, p. pgad361, 2023.